J Fluoresc (2015) 25:41–48
DOI 10.1007/s10895-014-1476-y

ORIGINAL PAPER

Aqueous Synthesis of Nontoxic Ag_2Se/ZnSe Quantum Dots Designing as Fluorescence Sensors for Detection of Ag(I) and Cu(II) Ions

Chunlei Wang · Shuhong Xu · Zengxia Zhao · Zhuyuan Wang · Yiping Cui

Received: 25 July 2014 / Accepted: 23 October 2014 / Published online: 14 November 2014
© Springer Science+Business Media New York 2014

Abstract We reported the synthesis of water-soluble and nontoxic Ag_2Se/ZnSe Quantum Dots (QDs) using for fluorescence sensors. The influences of various experimental conditions including the synthesis pH, types of ligand, feed ratios, and the refluxed time on the growth process and fluorescence of QDs were investigated in detail. Under optimal conditions, Ag_2Se/ZnSe QDs show a single emission peak around 490 nm with the maximal photoluminescence (PL) quantum yield (QYs) of 13.7 %. As-prepared Ag_2Se/ZnSe QDs can be used for detection of Ag(II) and Cu(II). The detection limits are 1×10^{-6} mol/L to 5×10^{-5} mol/L for Ag (I), and 2×10^{-6} mol/L to 1.10×10^{-4} mol/L for Cu(II).

Keywords Ag_2Se/ZnSe · Quantum dots · Fluorescence sensors

Introduction

Due to the high cytotoxicity of Cd-contained QDs, more attention has been paid to nontoxic Zn-contained QDs [1–3]. Since the emission of pure ZnSe QDs is located in the ultraviolet range, metal impurities are often added as dopant into crystalline of the ZnSe QDs to modulate the emission of ZnSe QDs into the visible range. Due to the lattice mismatch of the dopant with QDs, metal impurities tend to present on the surface of QDs. The PL of these surface doped QDs is easily quenched when QDs surface conditions change in different application surroundings [4]. To avoid the PL quenching, the impurities are required to dope inside QDs. In 2009, Zhang's group reported the first case of internally doped Cu:ZnSe and Mn:ZnSe QDs in aqueous solution [5]. They found that these water-soluble internally doped Cu:ZnSe QDs had extremely weak chemical stability in the open air due to the inevitable oxidation of mercapto-ligands by Cu impurities. This huge disadvantage makes these internally doped water-soluble Cu:ZnSe QDs impossible to apply in biology. Then, we reported the first example of water-soluble Cu:ZnSe/ZnS QDs with excellent stability [6]. The key for the excellent stability of as-prepared QDs is attributed to the simultaneous preparation of core-shell QDs and internally doped impurities. Although we improve the stability of water-soluble doped Cu:ZnSe QDs using ZnS shell, the preparation of shell in this paper is complex, and cost more materials. In addition, PL intensity of water-soluble doped ZnSe is weak. This would limit their development in application field. In this paper, Ag_2Se/ZnSe core-shell QDs have been synthesized. The prepared Ag_2Se/ZnSe QDs not only has good stability but also has better PL. Moreover, our QDs are synthesized in aqueous solution and do not contain toxic component. Thus, they can be used in sensitive sensors field. As we have known, there is no report on water-soluble Ag_2Se/ZnSe QDs using to detect Ag(I) and Cu(II) ions.

C. Wang · S. Xu · Z. Zhao · Z. Wang · Y. Cui (✉)
Advanced Photonics Center, School of Electronic Science and Engineering, Southeast University, Nanjing 210096, People's Republic of China
e-mail: cyp@seu.edu.cn

Experimental Section

Chemicals

All materials used in this work were analytical reagents. $Zn(NO_3)_2$ and $AgNO_3$ were purchased from Beijing Chemical Factory. $NaBH_4$ was purchased from Guangdong Chemical Reagent Engineering Technological Research and Development Center. NaOH was purchased from Shanghai Zhongshi Chemical Company. 3-Mercaptopropionic acid (MPA), 1-

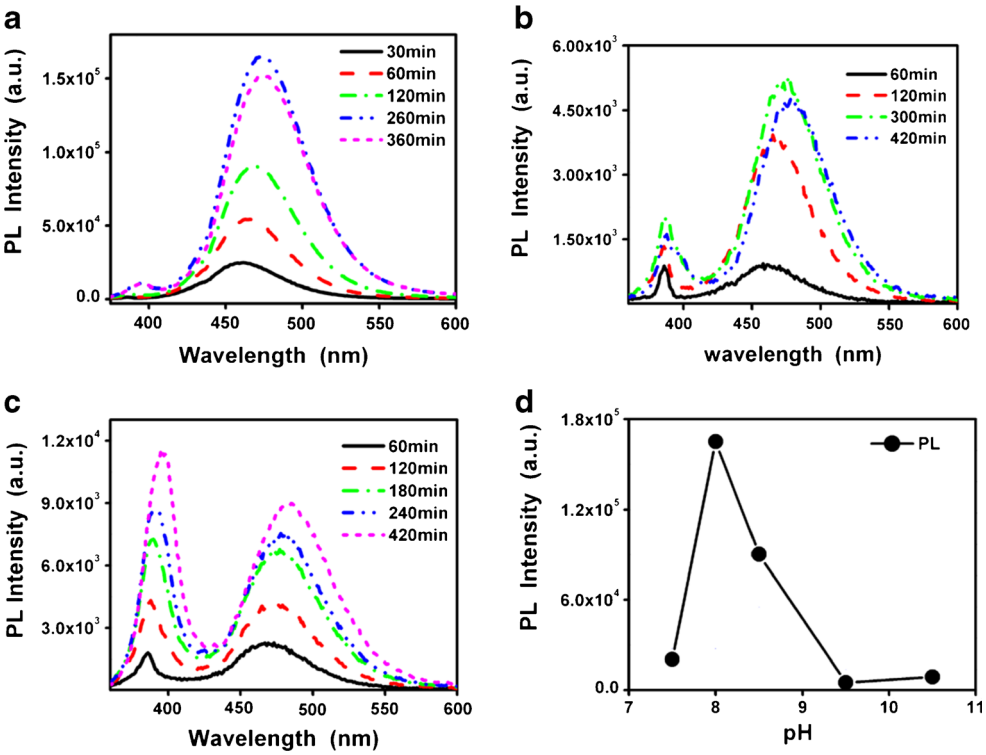

Fig. 1 PL of MPA-capped Ag_2Se/ZnSe QDs for pH values 8.0 (**a**) 9.5 (**b**) 10.5 (**c**) and the intensity of PL peaks of Ag_2Se/ZnSe QDs with optimal refluxed time at different pH (**d**)

thiolglycerol (TG), and Se powder were purchased from Aldrich. NaHSe solution was prepared by using Se with $NaBH_4$ according to the reference methods [7–9].

Synthesis of Core-Shell Ag_2Se/ZnSe QDs

The synthesis of Ag_2Se/ZnSe QDs contains two steps. The first one is formation of core Ag_2Se. Namely, the mixture of $AgNO_3$, and MPA was adjusted to pH 8.0 using NaOH solution. Freshly prepared NaHSe solution was injected into the mixture after the solution was aerated with N_2 for 30 min. The mixture was heated for 40 min and formed Ag_2Se core. Then, the addition of $Zn(NO_3)_2$ led to the growth of ZnSe shell. After refluxing for 6 h, Ag_2Se/ZnSe QDs were prepared. The total concentration of Zn in the mixture is 4×10^{-4} mol/L and the best feed ratio of Ag/Se/Zn/MPA was 1/2.5/5/120.

Table 1 The logarithmic value of negative dissociation constant (pK_a) for carboxyl group in MPA, hydroxyl group in TG, thiol groups in MPA (pK_{SH}), and the logarithmic value of negative solubility production constant for AgOH (pK_{sp})

Ligands or compound	*pKa* of terminal group	pK_{SH} of thiol group	solubility product (pK_{sp})
$HSCH_2CH_2COOH$ (MPA)	pK_{COOH} 4.32	10.84	—
$HSCH_2CHOHCH_2OH$ (TG)	pK_{OH} 9.43	–	—
AgoH	—	—	7.71

Characterization

UV–vis absorption spectra (UV) were recorded with a Shimadzu 3,600 UV–vis near-infrared spectrophotometer. Fluorescence experiments were performed with an Edinburgh FLS 920 spectrofluorimeter. The excitation wavelength was 350 nm, and the photon number of incidence is keeping at 3.55×10^5. The PL QY of QDs was estimated at room temperature with quinine in aqueous 0.5 mol/L H_2SO_4 as a standard PL reference (PL QY of 54.6 %) [10]. All optical measurements were performed at room temperature under ambient conditions. Transmission electron microscopy (TEM) and high-resolution (HR) TEM were recorded by a Tecnai F20 electron microscope with an acceleration voltage of 200 kV. The as-prepared Ag_2Se/ZnSe QDs were diluted for 20 times before dropping onto the Cu grid in TEM measurement. No post-synthesis treatment was applied to QDs before TEM measurement. X-ray photoelectron spectroscopy (XPS) was investigated by using a PHI550 spectrometer with an Mg Kα excitation (1253.6 eV). Binding energy calibration was based on SiO_2 at 103.0 eV. X-ray powder diffraction (XRD) investigation was carried out by using the D/max-2500/PC diffractometer with Cu Kα radiation (λ =0.15418 nm). For XPS and XRD measurements, Ag_2Se/ZnSe QDs powder was used. To obtain the powder, freshly prepared QDs were precipitated from the solution by the addition of equal volume of isopropanol, and then dried in vacuum.

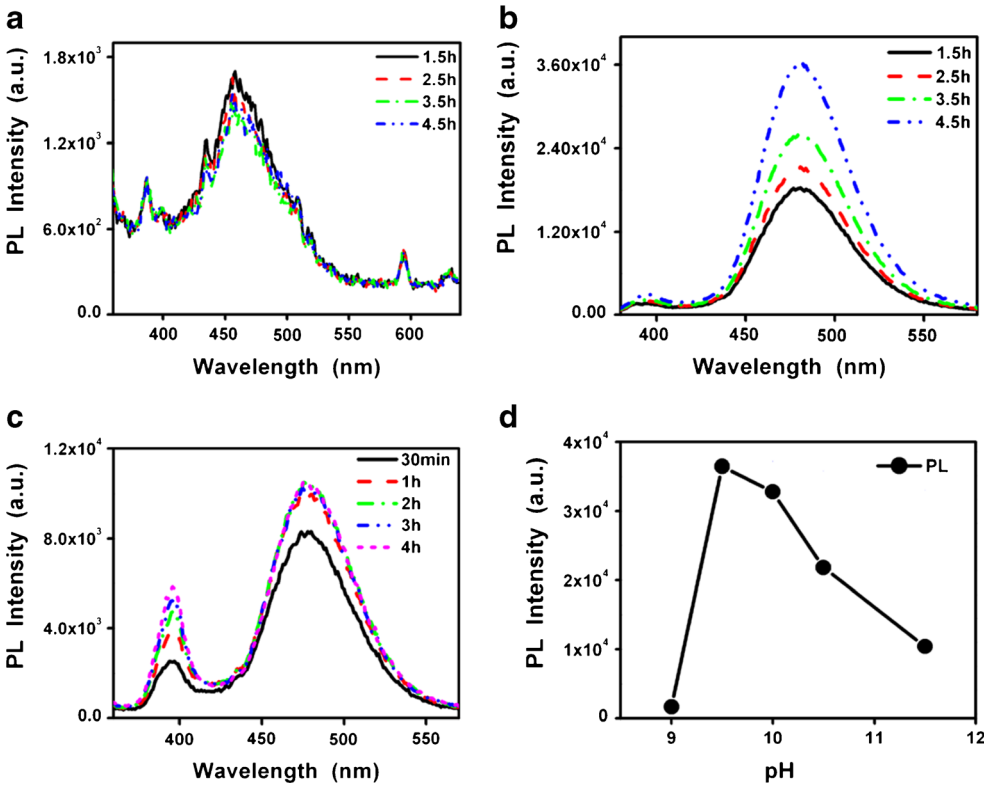

Fig. 2 PL of TG-capped Ag_2Se/ZnSe QDs for pH values 9.0 (**a**) 9.5 (**b**) 11.5 (**c**) and the intensity of PL peaks of Ag_2Se/ZnSe QDs with the optimal refluxed time at different pH (**d**)

Results and Discussion

Influence of pH Value and Ligand on the Fluorescence of Ag_2Se/ZnSe QDs

As we have known, pH value of mixing solution seriously affects the growth process and surface modification of QDs. In our previous work [11], we have investigated the pH-sensitive PL of various thiol ligand-capped CdTe QDs and established a general mechanism for pH-sensitive PL. In this work, we primarily studied the influence of pH on the growth and PL of core shell Ag_2Se/ZnSe QDs.

From the time-evolved PL of MPA-capped Ag_2Se/ZnSe QDs at pH 8.0 (Fig. 1a), the intensities of PL increase first and then decrease. There is an optimal refluxed time for MPA-capped Ag_2Se/ZnSe QDs. As for core-shell Ag_2Se/ZnSe QDs, the preparation contains two different stages: the formation of core Ag_2Se and the growth of ZnSe shell. Ag_2Se core are not luminescent. After the growth of ZnSe shell outside Ag_2Se core, luminescent core-shell Ag_2Se/ZnSe QDs formed. During the growth of ZnSe shell, Ag^+ and Zn^{2+} ions begin to diffuse into each other at the interface of core-shell, leading to different emission intensity for ZnSe QDs. Obviously, at the optimal refluxed time, the PL of Ag_2Se/ZnSe QDs has achieved the best. Proportion of Ag^+ and Zn^{2+} ions in Ag_2Se/ZnSe QDs at the moment is the most appropriate. If ZnSe shell keeps on growing outside Ag_2Se/ZnSe QDs, the PL of the QDs would decreased due to the increased interface stress and defects. Thus, refluxed time is the one factor that influences the PL intensity of Ag_2Se/ZnSe QDs.

As for samples synthesized at other pH values, we compared their maximal PL peaks intensity against pH as depicted in Fig. 1d. Obviously, the PL peaks intensity of the sample synthesized at pH 8.0 is the largest. When pH value is lower than 8.0, thiol ligands tend to detach from QD surface according to our previous work [11]. As seen from Table 1, the logarithmic value of negative dissociation constants (pK_a) for carboxyl group (−COOH) and thiol group (−SH) in MPA are 4.32 and 10.84. Thus, at pH over than 7.5, carboxyl group is completely ionized. There is no difference in carboxyl group in MPA for all samples in Fig. 1d. In comparison, the degree of ionization of thiol group is related to pH values at the current synthesis pH of QDs. At pH 8.0, the ionization of -SH is better than that at pH 7.5, resulting in better ligand modification and stronger PL for QDs. When the synthesis pH is over than 8.0, another effect appears beside aforementioned ionization of thiol group. As shown in Table 1, the logarithmic value of negative solubility product constant (pK_{sp}) for AgOH is 7.71. In our case, the feed concentration of Ag^+ is 8.36×10^{-4} mol/L, and hence the precipitation begins at pH 9.4 as calculated via the pK_{sp}. As shown by time-evolved PL of Ag_2Se/ZnSe QDs synthesized at pH 9.5 (Fig. 1b) and 10.5 (Fig. 1c), strong PL from band gap emission of ZnSe around

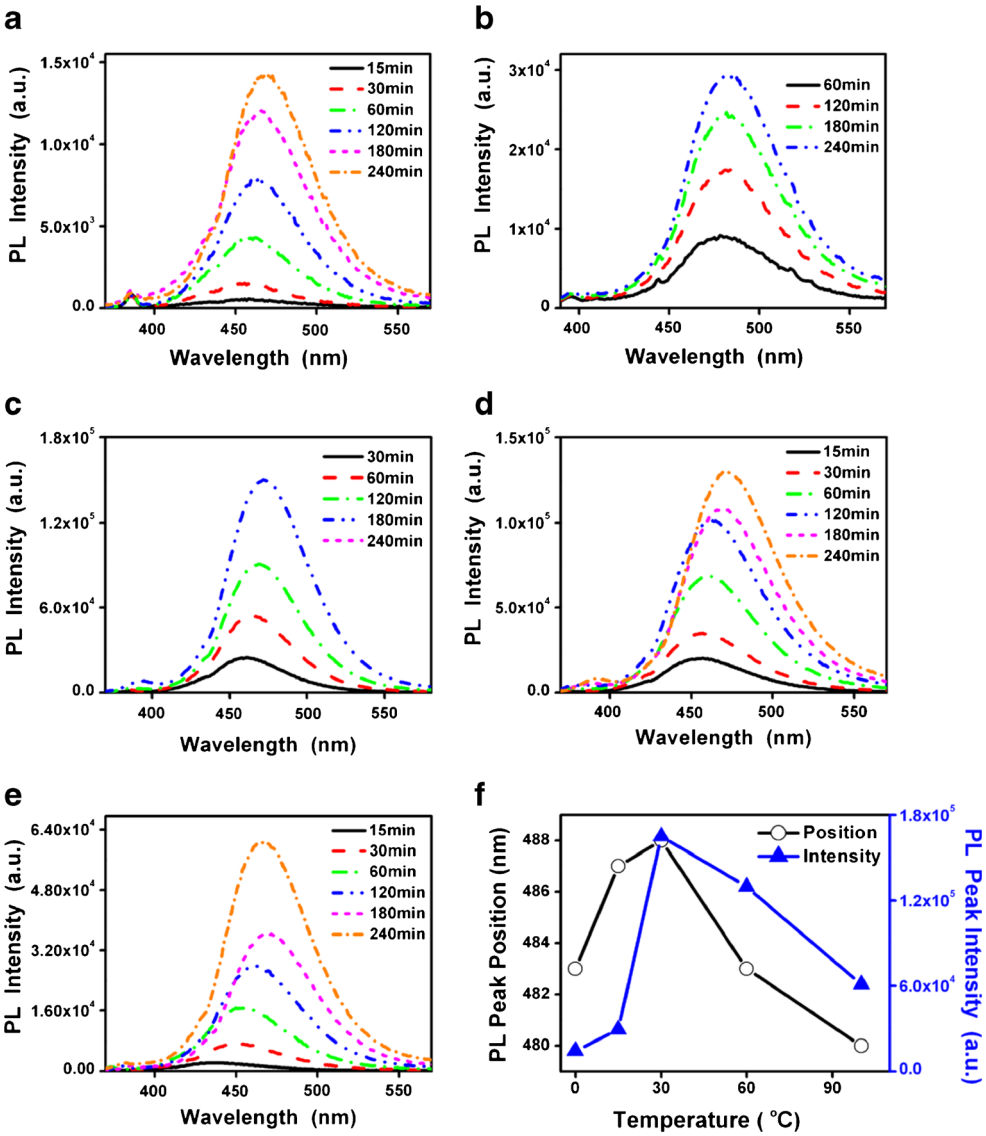

Fig. 3 PL of MPA-capped Ag_2Se/ZnSe QDs with the nucleation temperature 0 °C (**a**), 15 °C (**b**), 30 °C (**c**), 60 °C (**d**) and 100 °C (**e**). The intensity and position of PL peaks with different nucleation temperature

400 nm appears. Moreover, the intensity of ZnSe QDs at 400 nm is stronger at much higher synthesis pH values. It means that the formation of AgOH precipitation at high pH (such as 9.5 and 10.5) leads to less Ag_2Se in Ag_2Se/ZnSe QDs. As a result, the band gap emission of ZnSe at 400 nm cannot be fully suppressed.

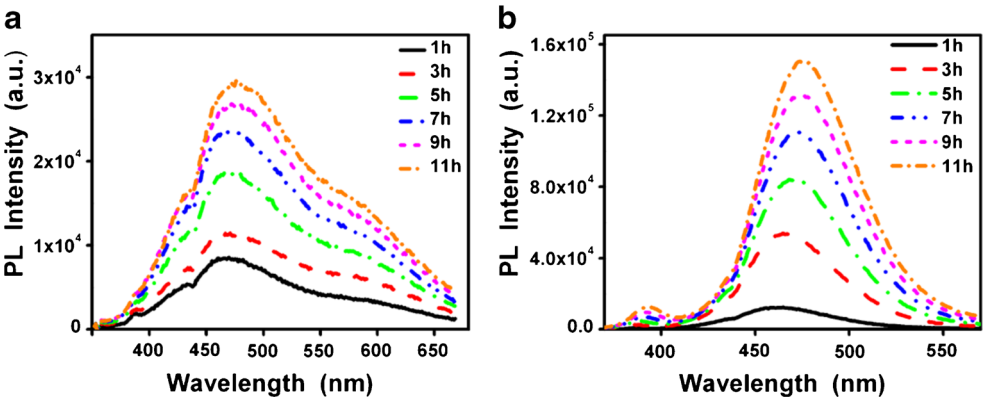

Fig. 4 PL of MPA-capped Ag_2Se/ZnSe QDs at Ag/Zn 1/50 (**a**) and 1/5 (**b**)

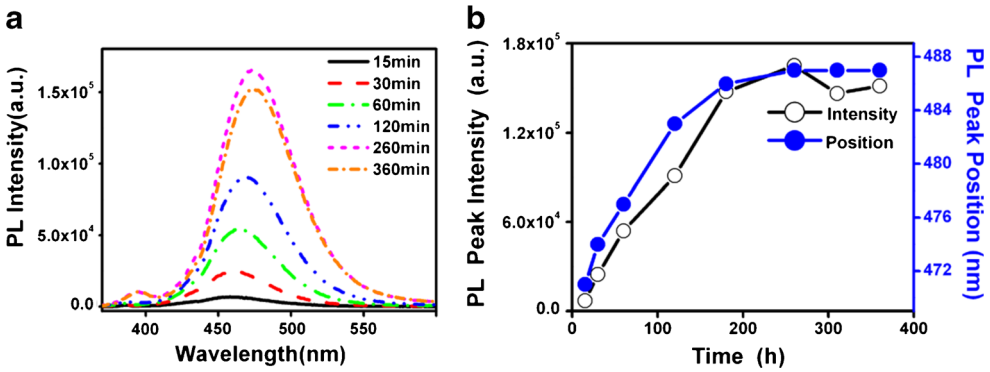

Fig. 5 PL of MPA-capped Ag_2Se/ZnSe QDs with different refluxed time (**a**) the intensity and position of PL peaks with different refluxed time (**b**)

In order to compare with the above analyses, we have prepared Ag_2Se/ZnSe QDs using TG as a ligand at pH 9.0, 9.5, 10.0, 10.5, and 11.5. Seeing from Fig. 2, the optimal pH for synthesis of TG-capped Ag_2Se/ZnSe QDs is 9.5, which is different with MPA-capped Ag_2Se/ZnSe QDs. From Table 1, we have known that the pK_a of hydroxyl group (−OH) in TG is 9.43 that is higher than that of carboxyl group in MPA. Thus, when pH values are lower than 9.43, TG-capped Ag_2Se/ZnSe QDs easily aggregate and lead to decreased PL intensity of QDs. Therefore, the optimal pH for the synthesis of TG-capped Ag_2Se/ZnSe QDs is 9.5.

In short, the influence of pH on Ag_2Se/ZnSe QDs is through pH-controlled ionizations of terminal group and thiol group as well as the formation of AgOH precipitation. These effects have different contributions to PL of Ag_2Se/ZnSe QDs at different pH ranges. The optimal pH is overall result of each factor.

Influence of the Nucleation Temperature on the Fluorescence of Ag_2Se/ZnSe QDs

As we have known that the temperature is important for the synthesis and growth of QDs. As for core-shell Ag_2Se/ZnSe QDs, their preparation has two different stages: the formation of core Ag_2Se and the growth of ZnSe shell. From our previous works, we have known that the best growing temperature of ZnSe is 100 °C. In the following, we mainly investigated the influence of nucleation temperature for core Ag_2Se (Fig. 3). The PL peaks intensity of Ag_2Se/ZnSe QDs at the same refluxed time of 240 min are 1.7×10^4, 3.1×10^4, 1.7×10^5, 1.3×10^5, and, 6.4×10^4 (a.u.) corresponding to the nucleation temperatures of 0, 15, 30, 60, and 100 °C. Obviously, the optimal nucleation temperature is 30 °C. It is well known that temperature plays an important role during the nucleation progress of QDs. With the optimal temperature QDs have good crystal, little defeat on the surface and high quantum yields [12]. In addition, we have found the PL peak positions are 488, 486, 487, 492 and 490 nm, which do not change seriously with the nucleation temperature. It illustrates that the nucleation temperature has little influence on the band structure of Ag-induced emission.

Influence of the Ratio of Ag/Zn and Zn/MPA on the Fluorescence of Ag_2Se/ZnSe QDs

The feed ratio has great influence on the growth and fluorescence of Ag_2Se/ZnSe QDs. In this paper, the concentration of Zn is constant. We investigated the fluorescence of Ag_2Se/ZnSe QDs at the ratio of Ag/Zn 1/50, 1/5, and 2/1 (Fig. 4).

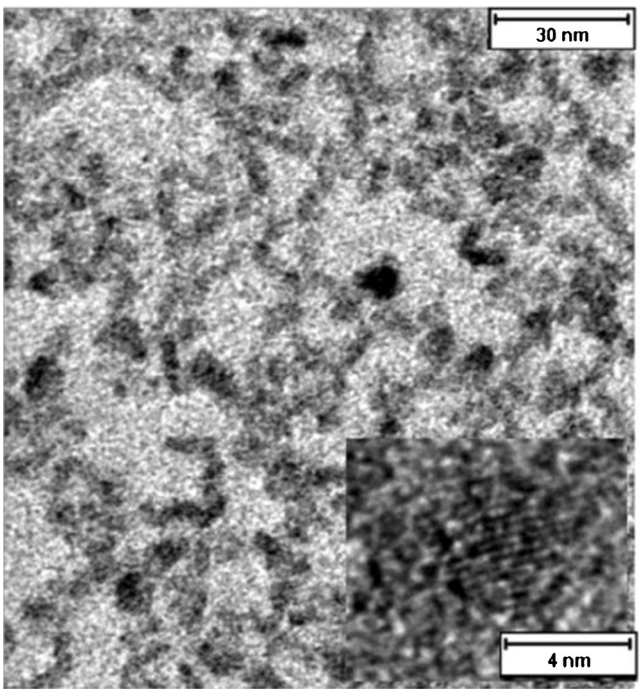

Fig. 6 TEM, and HRTEM (inset) of Ag_2Se/ZnSe QDs after refluxing for 4 h. The scale bars are 30 nm (TEM) and 4 nm (HRTEM)

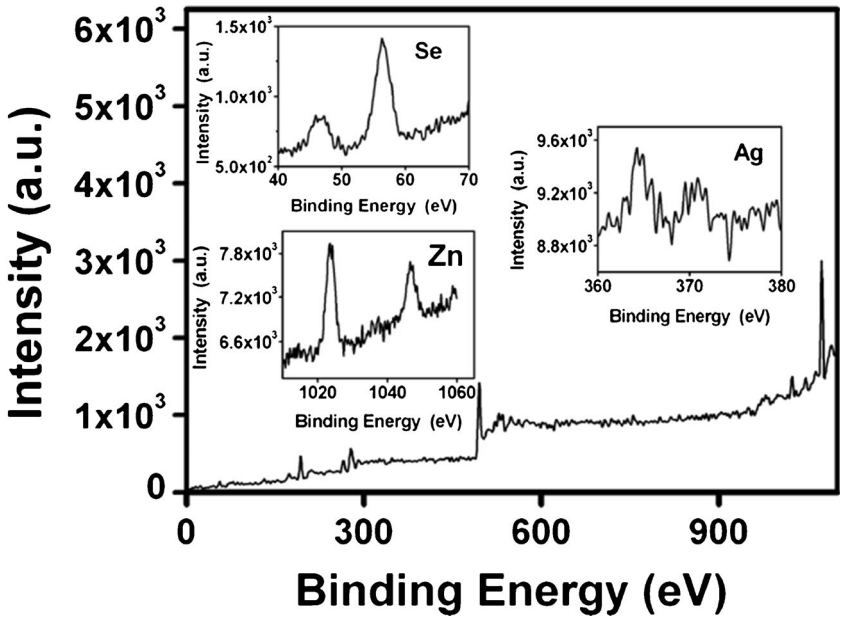

Fig. 7 XPS results of MPA-capped Ag_2Se/ZnSe QDs. The atomic ratios of Ag/Se/Zn were calculated according to the integrated intensity and the sensitivity factor of each element

As for the sample with Ag/Zn ratio of 1/50, the solution of sample before refluxing is colorless and transparent. After refluxing, the solution changes to a yellowish color with white emission under 365 nm UV irradiation. Seeing from Fig. 4a, the shape of the emission band is wider and gentle slope. The PL spectra of QDs have two emission bands: Ag-induced emission around 490 nm and the trap emission around 587 nm. Obviously, insufficient Ag at Ag/Zn ratio of 1/50 cannot fully suppress the trap emission. When the ratio of Ag/Zn is 1/5, plenty of Ag formed Ag_2Se core. From the PL spectra in Fig. 4b, only Ag-induced emission around 488 nm can be observed in the PL spectra of Ag_2Se/ZnSe QDs. The color of PL of Ag_2Se/ZnSe QDs is green under the irradiation of an UV lamp. For the sample with Ag/Zn of 2/1, the amount of Ag is over than NaHSe. There is no extra NaHSe to form ZnSe. Thus, $Zn(OH)_2$ precipitation can form outside Ag_2Se under alkaline solution[13]. Therefore, the precipitation is yellow-brown from the color of Ag_2Se.

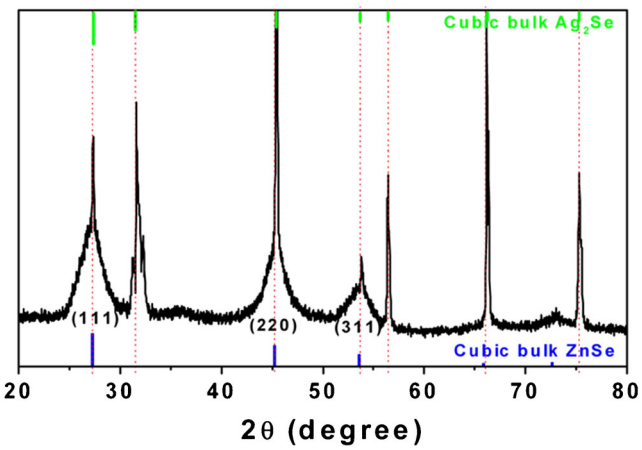

Fig. 8 XRD patterns of Ag_2Se/ZnSe QDs. The diffraction peaks of cubic bulk ZnSe and Ag_2Se are also marked by short lines

Characters of Core-Shell Ag_2Se/ZnSe QDs

With above experiments, we have confirmed the optimal synthesis conditions: namely the feed ratio of Ag/Se/Zn/MPA at 1/2.5/5/120, pH 8.0, and the nucleation temperature of 30 °C. PL intensity of the as-prepared Ag_2Se/ZnSe QDs increases first and then decreases with refluxed time (Fig. 5a). The optimal refluxed time is about 240 min. In this case, the maximal PL QYs of Ag_2Se/ZnSe QDs are measured as 13.7 % in comparison to quinine in 0.5 mol/L H_2SO_4. The

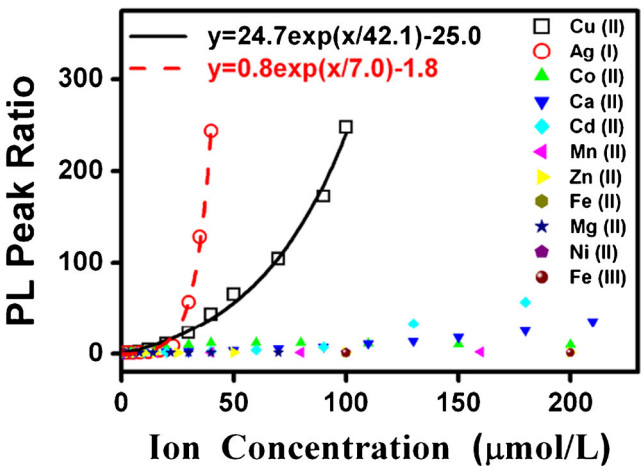

Fig. 9 The PL peak intensity ratios of Ag_2Se/ZnSe QDs without and with addition of various ions versus the concentration of addition ions. The signals of Cu(II) and Ag(I) were fitted by exponential equations with goodness of fitting over than 0.99

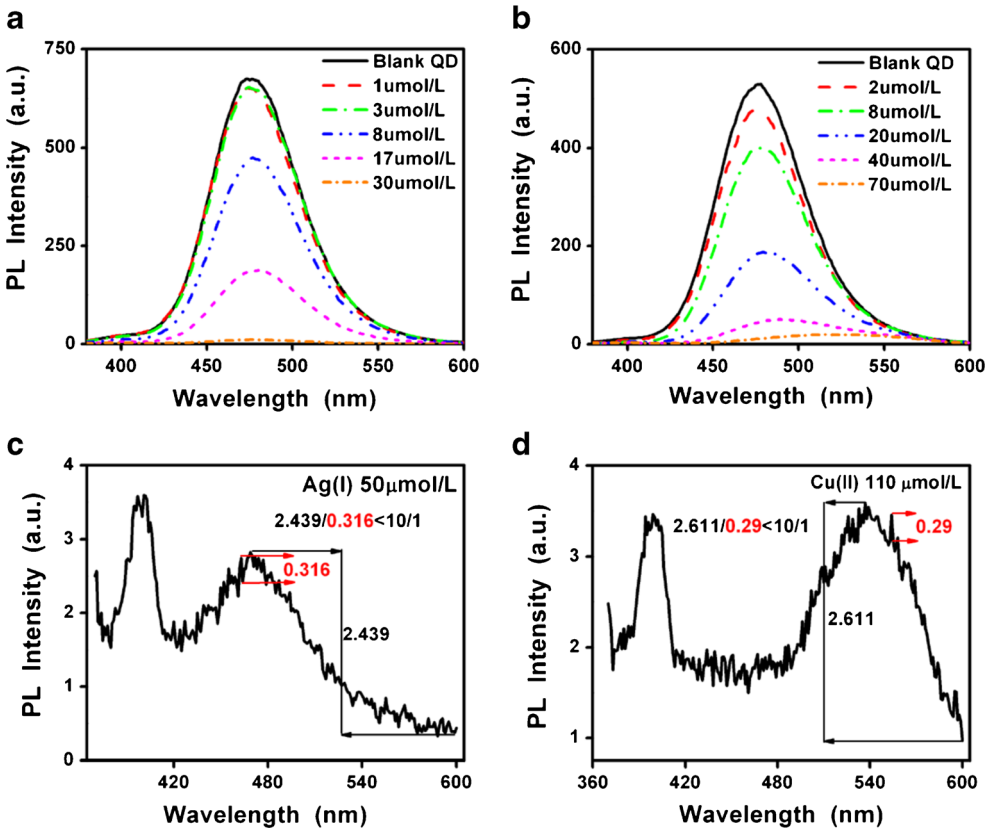

Fig. 10 PL spectra of Ag_2Se/ZnSe QDs fluorescence sensors after addition of different concentrations of Ag(I) (**a**) and Cu(II) (**b**) ions. The signal-to-noise of PL spectra after addition of 5.5×10^{-5} mol/L Ag(I) (**c**) and 1.1×10^{-4} mol/L Cu(II) (**d**) ions

position of PL peak shifts to the red with refluxed time. The Stokes shift is about 90 nm, suggesting the emission of Ag_2Se/ZnSe QDs from Ag impurity energy level intermediate the forbidden band of ZnSe.

As shown by TEM image in Fig. 6, the size of MPA-capped Ag_2Se/ZnSe QDs is about 6 nm. HRTEM image show obvious interface between the core and the shell. XPS results confirm the existence of Zn^{2+}, Se^{2-} and Ag^{+} inside QDs (Fig. 7). The ratio of Ag/Se/Zn in Ag_2Se/ZnSe QDs is measured as 4.93/3.32/1.00, corresponding to $(Ag_2Se)_2ZnSe$, suggested the formation of extremely thick ZnSe shell outside the core. XRD in Fig. 8 also confirms the formation of a core-shell structure. There are two kinds of diffraction peaks: namely wide peaks and narrow peaks. Wide peaks have the same diffractive angles with cubic bulk ZnSe. Narrow peaks correspond to cubic bulk Ag_2Se. It illustrates the existing of cubic ZnSe and Ag_2Se in Ag_2Se/ZnSe QDs. Generally speaking, as for core-shell QDs, they only have diffractive peaks of the core [14, 15]. In Ag_2Se/ZnSe QDs, there are diffractive peaks for cubic ZnSe and Ag_2Se at the same time. The possible reason is the extremely large lattice mismatch between ZnSe and Ag_2Se as well as the extremely thick ZnSe shell (XPS results) leading to large lattice stress between the core and the shell. As a result, ZnSe shell grows via the lattice itself rather than along the lattice of Ag_2Se core. This is also the reason why we can see obvious core-shell interface.

The Application of Ag_2Se/ZnSe QDs: Sensitivity of QDs Fluorescence Sensors to Metal Ions

The as-prepared Ag_2Se/ZnSe QDs possess good PL stability, biocompatibility, and low cytotoxicity, and thus can be used in many fields such as solar cell, fluorescence encoding and sensors. In the following, we applied Ag_2Se/ZnSe QDs in ionic probing.

Freshly prepared MPA-capped Ag_2Se/ZnSe QDs were used as fluorescence probing. Various ions including Ag(I), Ca(II), Cd(II), Co(II), Cu(II), Fe(II), Fe(III), Mn(II), Mg(II), Zn(II), and Ni(II) were added into Ag_2Se/ZnSe QDs under vigorous stirring. PL spectra were used for monitoring the impact of various ions. Since the PL of QDs changed with pH value, we used the ratio of PL peak intensity of QD without and with target ions to exclude the influence of pH on the PL [16]. In this way, the alteration of the PL ratio is only caused by the different sensitivity of the QDs to the ion.

From Fig. 9, it can be seen that QDs are sensitive to Ag(I) and Cu(II) ions. The measured PL ratios against ion concentration can be fitted well by exponential equations as shown in Fig. 9. Since all the measured data locate in the exponential equation, it cannot fix the detection limit from the discrete degree between the measured data and the exponential equation. It also means the lowest and highest detection limits should be fixed by some other methods. In this work, we

fixed the lowest detection limits of metal ion by using the PL ratio of 0.95 after addition of ions into QDs. When the preserved PL ratio is high than 0.95, it is difficult to discriminate the PL spectra between the blank sample and the target sample, and it is considered not suitable for accurate detection. According to Fig. 10a and b, the lowest detection limit of Ag(I) and Cu(II) are 1×10^{-6} mol/L and 2×10^{-6} mol/L, respectively. In comparison, the highest detection limits of metal ion are fixed by using the signal-to-noise of PL of 10/1. According to Fig. 10c and d, the highest detection limits of Ag(I) and Cu(II) are 5.5×10^{-5} mol/L and 1.1×10^{-4} mol/L.

Conclusions

In conclusion, we reported the first example of nontoxic Ag_2Se/ZnSe QDs as fluorescence sensors. As-prepared Ag_2Se/ZnSe QDs are about 6 nm, with maximal PL QY of 13.7 %. The influence of pH, nucleation temperature, the ratio of Ag/Zn on PL and growth of Ag_2Se/ZnSe QDs has been investigated. As-prepared Ag_2Se/ZnSe QDs were used to detect metal ions via their fluorescence sensors. The detection limits of Ag(I) are 1×10^{-6} mol/L to 5×10^{-5} mol/L, of Cu(II) are 2×10^{-6} mol/L to 1.10×10^{-4} mol/L.

Acknowledgments This work is supported by the National Key Basic Research Program of China (Grant No. 2015CB352002), National Natural Science Foundation of China (Grant Nos. 61475034, 21104009, 21403034, 61177033), the Fundamental Research Funds for the Central Universities (No. 2242014R30006), the natural science foundation of Jiangsu Province Youth Fund (No. BK20140650).

References

1. Wang C, Zhang H, Zhang J, Li M, Sun H, Yang B (2007) J Phys Chem C 111:2465–2469
2. Derfus AM, Chan WCW, Bhatia SN (2004) Nano Lett 1:11–18
3. Murray CB, Norris DJ, Bawendi MG (1993) J Am Chem Soc 115: 8706
4. Ladizhansky V, Hodes G, Vega S (1998) J Phys Chem B 102:8505–8509
5. Pradhan N, Goorskey D, Thessing J, Peng X (2005) J Am Chem Soc 127:17586–17587
6. Xu SH, Wang CL, Wang ZY, Zhang HS, Yang J, Xu QY, Shao HB, Li RQ, Lei W, Cui YP (2011) Nanotechnology 22:275605
7. Han J, Zhang H, Tang Y, Liu Y, Yao X, Yang B (2009) J Phys Chem C113:7503–7510
8. Zhang H, Liu Y, Wang C, Zhang J, Sun H, Li M, Yang B (2008) ChemPhysChem 9:1309–1316
9. Xu SH, Wang CL, Xu QY, Zhang H, Li RQ, Shao HB, Lei W, Cui YP (2010) Chem Mater 22:5838–5844
10. Xu SH, Wang CL, Xu Q, Li RQ, Shao HB, Zhang H, Fang M, Lei W, Cui YP (2010) J Phys Chem C 114:14319–14326
11. Xu SH, Wang CL, Zhang H, Wang ZY, Yang B, Cui YP (2011) Nanotechnology 22:315703
12. Gerion D, Parak WJ, Williams SC, Zanchet D, Micheel CM (2002) J Am Chem Soc 24:7070–7074
13. Xu S, Wang C, Xu Q, Zhang HS, Li RQ, Shao HB, Lei W, Cui YP (2010) Chem Mater 22:5838–5844
14. Hines MA, Guyot SP (1996) J Phys Chem 100:468–471
15. Li JJ, Wang YA, Guo WZ (2003) J Am Chem Soc 125:12567–12575
16. Xu S, Wang C, Xu Q, Zhang HS, Sun QF, Wang ZY, Cui YP (2012) J Mater Chem 22:9216–9221